2015

Analysis of critically refracted longitudinal waves

Ning Pei
Iowa State University

Leonard J. Bond
Iowa State University, bondlj@iastate.edu

Analysis of critically refracted longitudinal waves

Abstract

Fabrication processes, such as, welding, forging, and rolling can induce residual stresses in metals that will impact product performance and phenomena such as cracking and corrosion. To better manage residual stress tools are needed to map their distribution. The critically refracted ultrasonic longitudinal (LCR) wave is one such approach that has been used for residual stress characterization. It has been shown to be sensitive to stress and less sensitive to the effects of the texture of the material. Although the LCR wave is increasingly widely applied, the factors that influence the formation of the LCR beam are seldom discussed. This paper reports a numerical model used to investigate the transducers' parameters that can contribute to the directionality of the LCR wave and hence enable performance optimization when used for industrial applications. An orthogonal test method is used to study the transducer parameters which influence the LCR wave beams. This method provides a design tool that can be used to study and optimize multiple parameter experiments and it can identify which parameter or parameters are of most significance. The simulation of the sound field in a 2-D "water-steel" model is obtained using a Spatial Fourier Analysis method. The effects of incident angle, standoff, the aperture and the center frequency of the transducer were studied. Results show that the aperture of the transducer, the center frequency and the incident angle are the most important factors in controlling the directivity of the resulting LCR wave fields.

Keywords

Ultrasonics, Numerical methods, Wave mechanics, Corrosion, Educational assessment, Fourier analysis, Welding

Disciplines

Manufacturing | Mechanics of Materials

Analysis of critically refracted longitudinal waves

Cite as: AIP Conference Proceedings **1650**, 1805 (2015); https://doi.org/10.1063/1.4914805
Published Online: 02 April 2015

Ning Pei, and Leonard J. Bond

Analysis of Critically Refracted Longitudinal waves

Ning Pei[1,a)] and Leonard J.Bond[1)]

[1]*Center for Nondestructive Evaluation*
Iowa State University
Ames, IA 50011

a)Corresponding author: npei@iastate.edu

Abstract. Fabrication processes, such as, welding, forging, and rolling can induce residual stresses in metals that will impact product performance and phenomena such as cracking and corrosion. To better manage residual stress tools are needed to map their distribution. The critically refracted ultrasonic longitudinal (LCR) wave is one such approach that has been used for residual stress characterization. It has been shown to be sensitive to stress and less sensitive to the effects of the texture of the material. Although the LCR wave is increasingly widely applied, the factors that influence the formation of the LCR beam are seldom discussed. This paper reports a numerical model used to investigate the transducers' parameters that can contribute to the directionality of the LCR wave and hence enable performance optimization when used for industrial applications. An orthogonal test method is used to study the transducer parameters which influence the LCR wave beams. This method provides a design tool that can be used to study and optimize multiple parameter experiments and it can identify which parameter or parameters are of most significance. The simulation of the sound field in a 2-D "water-steel" model is obtained using a Spatial Fourier Analysis method. The effects of incident angle, standoff, the aperture and the center frequency of the transducer were studied. Results show that the aperture of the transducer, the center frequency and the incident angle are the most important factors in controlling the directivity of the resulting LCR wave fields.

INTRODUCTION

Residual stresses [1-2] are self-equilibrating forces which can be generated during fabrication processes, such as, welding, forging, or rolling, such as is shown in Fig. 1. These forces are stress which exists in an elastic solid body in the absence of, or in addition to, the stresses caused by an external load. Residual stresses in the material can be either compressive or tensile in different regions. Compressive residual stresses are generally useful while tensile residual stresses are generally detrimental. Examples of processes which can induce beneficial stress include shot peening and shrinking. To better utilize and manage stress it is necessary to have tools that can be used to map stress fields, both on the surface and within a part.

A lot of methods have been used to measure stress [3] including X-ray diffraction and strain gages with hole drilling. Such techniques in the first case require expensive equipment and in the second are only applied at or near a surface, and are not nondestructive [4]. Among the nondestructive methods for mapping stresses available are those which use ultrasonic measurements. Both the velocity and the stress are determined by the elastic constants of a solid [5].

Ultrasonic methods [6, 7] have been demonstrated to be an effect measurement modality: they are nondestructive, they can be relatively inexpensive, and easy to perform. There are some challenges faced in providing the needed precision for accurate stress determination at low loads. Such methods do consider the changes in velocity (elastic

41st Annual Review of Progress in Quantitative Nondestructive Evaluation
AIP Conf. Proc. 1650, 1805-1814 (2015); doi: 10.1063/1.4914805

constants), and this is also sensitive to the composition, grain size, texture and temperature of the material. One ultrasound approach is to use longitudinal critically refracted (LCR) waves, which are also referred to as creeping waves in some of the literature [8]. For a fluid loaded surface the LCR wave is generated at the first critical angle of the incident longitudinal wave, which gives waves that propagate below, yet close to the surface of the specimen. It is found that for residual stress detection, the LCR wave has some advantages: it is relatively sensitive to the effects of residual stress, and it is less sensitive to the structure of materials [9] and the application of LCR waves for residual stress detection has been considered by several groups. [10-14]

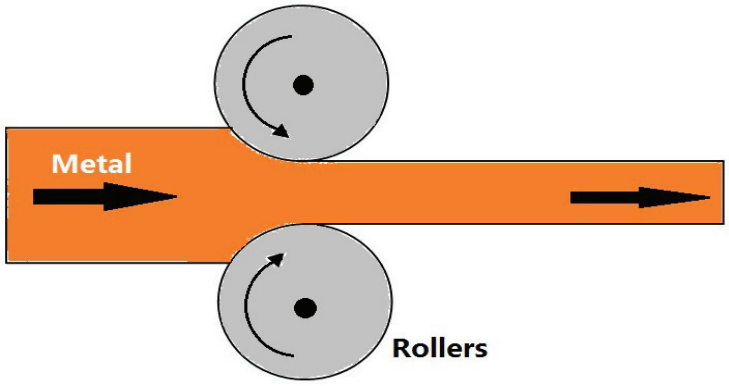

FIGURE 1. Schematic of rolling process, which can induce residual stress in steel.

Theoretical analysis of LCR waves was provided by Basatskaya and Ermolov [15] in 1981. They began from the basic wave equations and boundary conditions and established a 2-D model for harmonic waves. The directionality of the LCR wave is calculated and the depth to which it can spread is discussed. The typical sound field of the LCR wave was calculated by Langenberg et al [8] in 1990, where they used a numerical elastodynamic finite integration method. Since then, it seems that there are limited research work on more fundamental aspects of this family of waves.

In the current paper the analysis of LCR waves is based on the calculation of the sound field, using a numerical integration method. After obtaining the sound field of the LCR wave, the characterization of this wave can be discussed. Directivity is one of the most important parameters and only after analysis of the directivity can we know where the energy of the LCR wave is concentrated. What's more, it is very helpful to know both its spread with depth and its directivity. Prior work has shown that the parameters that control the directivity of the LCR wave include the transducer frequency, the aperture, the distance from the transducer to the surface, the incident angle and material in which waves are generated. The Orthogonal Experiment Design Method [16-18] is used for data analysis.

THE GENERATION OF LCR WAVES

When ultrasound is transmitted from one medium to another, reflection and refraction will occur. For example, when a longitudinal wave is transmitted from water to steel, both longitudinal and transverse waves will be generated in the steel. The angles for the transmitted waves follow Snell's law:

$$\frac{C_{L1}}{\sin\alpha} = \frac{C_{L2}}{\sin\beta_L} = \frac{C_{S2}}{\sin\beta_S} \tag{1}$$

where C_{L1} is the longitudinal velocity in the water, C_{L2} and C_{S2} are the longitudinal and transverse velocities respectively in the steel. According to Snell's law, as the incident angle, α, increases the refraction angle will reach 90°. When β_L reaches 90°, it is called the first critical angle and a wave knows as the LCR or creeping wave forms, as shown in Fig. 2. In principal this LCR or creeping wave propagates parallel to the interface of water and steel, but in reality the wave is transmitted at an angle to the interface.

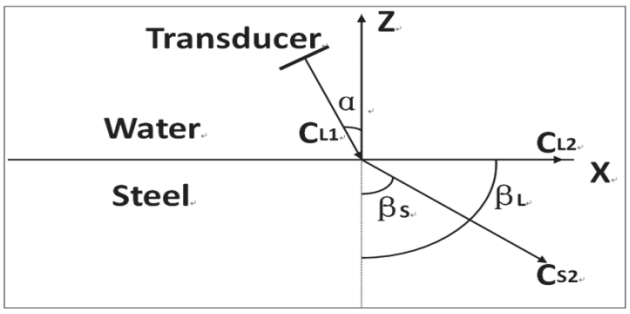

FIGURE 2. The generation of LCR waves.

THE ACOUSTIC FIELD OF THE LCR WAVE

It can be shown how the acoustic field will develop [19-20]. When considered in a 2D model, the wave equation can be described by a scalar potential $\varphi(x,z,t)$ and a vector potential $\psi(x,z,t)$:

$$\nabla^2\varphi = \frac{1}{C_L^2}\ddot{\varphi} \tag{2}$$

$$\nabla^2\vec{\psi} = \frac{1}{C_L^2}\vec{\psi} \tag{3}$$

Applying a Fourier transform to both space (x) and time (t), in the scalar potential $\varphi(x,z,t)$:

$$\varphi^*(k_x,z,\omega) = \frac{1}{2\pi}\int_{-\infty}^{+\infty}\varphi(x,z,t)e^{-j\omega t}e^{-jk_x x}dxdt \tag{4}$$

$$\varphi^*(k_x,z,\omega) = Ae^{-k_{f1}z} + Be^{k_{f1}z} \tag{5}$$

where $k_{f1} = \sqrt{\omega^2/C_L^2 - k_x^2}$

It is the same for vector potential $\vec{\psi}(x,z,t)$ and $\vec{\psi}^*(x,z,t)$:

$$\vec{\psi}^*(k_x,z,\omega) = \frac{1}{2\pi}\int_{-\infty}^{+\infty}\vec{\psi}(x,z,t)e^{-j\omega t}e^{-jk_x x}dxdt \tag{6}$$

$$\psi^*(k_x,z,\omega) = Ce^{-k_{f2}z} + De^{k_{f2}z} \tag{7}$$

where $k_{f2} = \sqrt{\omega^2/C_T^2 - k_x^2}$

For the solid, the potential function can be expressed as:

$$\varphi^*(k_x,z,\omega) = T_1e^{-jk_cz} \tag{8}$$

$$\vec{\psi}^*(k_x,z,\omega) = T_2e^{-jk_sz} \tag{9}$$

where T_1 and T_2 are the transmission coefficients, and $k_c = \sqrt{\omega^2/v_c^2 - k_x^2}$, $k_s = \sqrt{\omega^2/v_s^2 - k_x^2}$

According to the relationship of the potential and the displacement $\vec{u} = \nabla\varphi + \nabla\times\psi$, the normal displacement in the solid can be expressed as:

$$\vec{u}_z^*(k_x,z,\omega) = -jk_cT_1e^{-jk_cz} + jk_sT_1e^{-jk_sz} \tag{10}$$

According to the relationship between stress and strain and the relationship between strain and displacement, the normal stress in the solid can be written as:

$$\vec{\sigma}_{zz}^*(k_x,z,\omega) = (2\mu k_x^2 - \rho_2\omega^2)T_1e^{-jk_cz} + 2\mu k_xk_sT_2e^{-jk_sz} \tag{11}$$

To simplify the model (Fig. 3), the acoustic pressure from the transducer can be projected to the interface of the water and the solid (steel), and then the excitation on this interface could be defined as an applied stress σ_{22}, which can be expressed as:

$$\sigma_{zz/z=0} = \begin{cases} A\exp[i(k^{'}\sin\theta - \omega t)], for\ |x| \le d; \\ 0 \qquad\qquad\quad , for\ |x| > d; \end{cases} \tag{12}$$

where A is the excitation amplitude; $d = \frac{1}{2}D/\cos\theta$, D is the diameter of the transducer; $k^{'} = \frac{\omega}{c^{'}}$; $c^{'}$ is the velocity of the water; ω is the angular frequency.

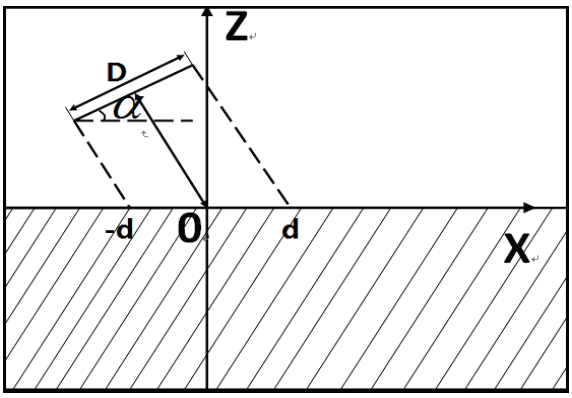

FIGURE 3. Schematic for simulating LCR wave.

THE IMAGE OF THE ACOUSTIC FIELD

The simulation of the acoustic field of LCR wave is calculated using MATLAB. The parameters that were used are shown in the Table 1.

TABLE 1. Material properties of water and steel.

Material	**Density**(g/cm^3)	**Longitudinal Velocity**(m/s)	**Transversal Velocity**(m/s)
Water	1.0	1487	---
Steel	7.8	5940	3230

The acoustic wave field including the longitudinal, transverse and head waves in the steel is shown in Fig. 4. To satisfy the bound conditions, the head wave and transverse wave are always linked to each other at the interface.

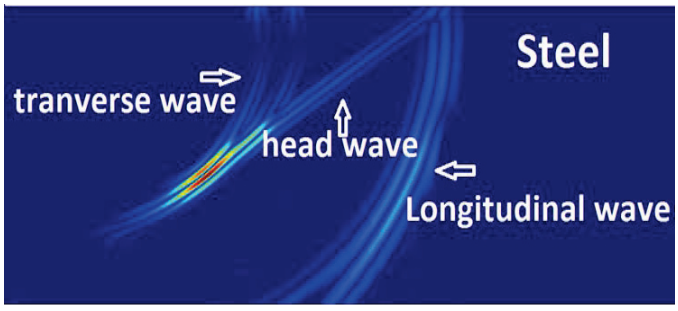

FIGURE 4. An example of the acoustic field including the LCR wave.

In addition to the wave field point displacement (RF wave forms) were calculated. An example of a typical displacement signal calculated for a point in the steel, is shown as Fig. 5. It clearly shows the longitudinal, head and transverse waves and their relative amplitudes, shown as if measured and given as voltages from a pinducer (point receiver). The results of the new model were found to be in good general agreement with the study published by Belgroune et al [20], however in that published paper not all parameters are provided, so an exact comparison for the case of an identical configuration was not possible.

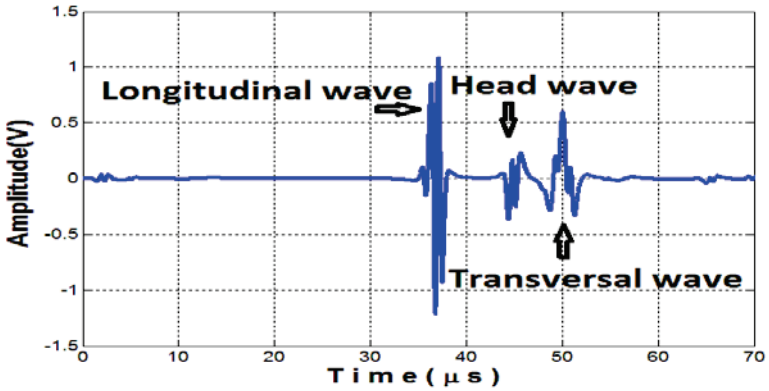

FIGURE 5. Typical received signal in the steel.

THE ANALYSIS OF PARAMETERS THAT CONTROL THE DIRECTIVITY OF THE LCR WAVE

The new model reported above was used to simulate and investigate the effects of various parameters on the resulting wave fields. A sensitivity analysis was performed. The signals were calculated and assumed to be received at points on a 90 degree arc with its center at the point of incidence for the transducers central ray onto the interface, as shown in Fig. 6. The receiving distance, L, from the point on the interface is 60mm.

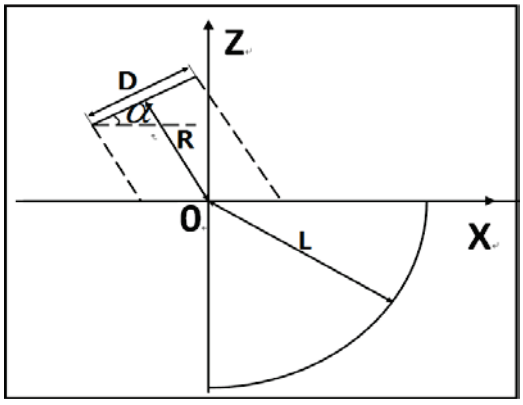

FIGURE 6. Schematic diagram of the model.

The amplitude of the LCR wave at different locations on the arc was used to plot the directivity of the LCR wave. A comparison of the directivity of the LCR wave obtained by this model with that for the best estimate of the corresponding case shown in the literature [21] are presented in Fig. 7. The current data, and that from the literature are seen to be in general agreement, in terms of both magnitude and angle.

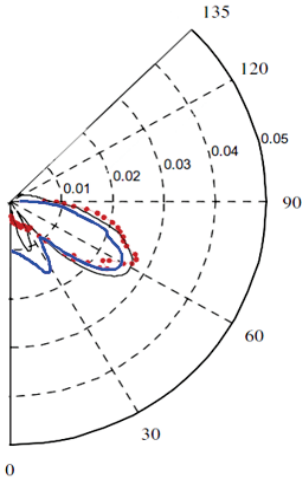

FIGURE 7. Comparison of the LCR wave from the literature and that from the current model: current study – blue curve and corresponding data from the literature [21] – black curve and red dot.

The frequency, the aperture, the incident angle, the distance from the transducer to the interface (R) and the receiving locations (L) were all varied to enable their effects on the directivity of the LCR wave to be estimated. The values of these parameters, for three cases, are shown in Table 2.

TABLE 2. The values of the parameters for three example configurations.

	F(frequency: MHz)	**D**(mm)	α (angle: degree)	**R**(mm)	**L**(mm)
1	1.75	6	13.5	15	50
2	2	7	14.5	22	60
3	2.25	8	15.5	30	70

The Orthogonal Experiment Method is used for the analysis of the effects of the variation of these parameters on the resulting data. The Orthogonal Experiment Method is used to study the effects on a system when more than two parameters are involved and to try to provide a sensitivity analysis using an optimized set of simulations (or experiments). The Orthogonal Experiment Table used for different application is given as Table 3 and in this case, L_3^{27} is used.

TABLE 3. Orthogonal Experiment Table of L_3^{27}.

Num	**F**	**D**	**F*D_1**	**F*D_2**	α	**R**	**L**	**Error**					
	1	**2**	**3**	**4**	**5**	**6**	**7**	**8**	**9**	**10**	**11**	**12**	**13**
1	1	1	1	1	1	1	1	1	1	1	1	1	1
2	1	1	1	1	2	2	2	2	2	2	2	2	2
3	1	1	1	1	3	3	3	3	3	3	3	3	3
4	1	2	2	2	1	1	1	2	2	2	3	3	3
5	1	2	2	2	2	2	2	3	3	3	1	1	1
6	1	2	2	2	3	3	3	1	1	1	2	2	2
7	1	3	3	3	1	1	1	3	3	3	2	2	2
8	1	3	3	3	2	2	2	1	1	1	3	3	3
9	1	3	3	3	3	3	3	2	2	2	1	1	1
10	2	1	2	3	1	2	3	1	2	3	1	2	3
11	2	1	2	3	2	3	1	2	3	1	2	3	1
12	2	1	2	3	3	1	2	3	1	2	3	1	2
13	2	2	3	1	1	2	3	2	3	1	3	1	1

14	2	2	3	1	2	3	1	3	1	2	1	2	2
15	2	2	3	1	3	1	2	1	2	3	2	3	3
16	2	3	1	2	1	2	3	3	1	2	2	3	2
17	2	3	1	2	2	3	1	1	2	3	3	1	3
18	2	3	1	2	3	1	2	2	3	1	1	2	1
19	3	1	3	2	1	3	2	1	3	2	1	3	1
20	3	1	3	2	2	1	3	2	1	3	2	1	2
21	3	1	3	2	3	2	1	3	2	1	3	2	3
22	3	2	1	3	1	3	2	2	1	3	3	2	2
23	3	2	1	3	2	1	3	3	2	1	1	3	3
24	3	2	1	3	3	2	1	1	3	2	2	1	1
25	3	3	2	1	1	3	2	3	2	1	2	1	1
26	3	3	2	1	2	1	3	1	3	2	3	2	2
27	3	3	2	1	3	2	1	2	1	3	1	3	3

(**F*D_1 and F*D_2 are two interaction effect of F and D**)

As to the Orthogonal Experiment Method, Range Analysis and Analysis of Variance are two typical data analysis methods: Range Analysis is used to order the parameters' importance while Analysis of Variance is necessary to make sure whether the result has statistical significance.

TABLE 4. Analysis of Variance of the result.

Source	Type Ⅲ Sum of Squares	df	Mean Square	F	Sig.
Corrected Model	626.3[a]	14	44.74	41.65	.000
Intercept	79489.81	1	79489.81	7.401E4	.000
F	98.74	2	49.37	45.966	.000
D	180.96	2	90.48	84.241	.000
F*D_1	11.19	2	5.59	5.207	.024
F*D_2	2.3	2	1.15	1.069	.374
Angle	324.52	2	162.26	151.069	.000
R	3.19	2	1.59	1.483	.266
L	5.41	2	2.7	2.517	.122
Error	12.89	12	1.07		
Total	80129	27			
Corrected Total	639.19	26			

a. R Squared= .980 (Adjusted R Squared = .956)

The results of the Analysis of Variance are shown as Table 4. These data are obtained using SPSS [22] (SPSS is a statistic software that can be used for data analysis). It is shown that F, D, F*D_1and Angle are the main parameters and their significant are all less than 0.005. Corrected Model should less than 0.005 ("0.005" is a defined parameter to judge the result [22]), that's to say the result has statistic meaning and is reliable.

TABLE 5. Range Analysis of the result.

	F	D	F*D_1	Angle
Mean value 1	51.667	51.000	54.111	49.778
Mean value 2	54.899	54.444	53.556	54.778
Mean value 3	56.222	57.333	55.111	58.222
Range	4.555	6.333	1.555	8.444

The Range Analysis of the results are given in Table 5. Based on the Range data in Table 5, the significance order for the key parameters are Angle>D>F>F*D_1(Interaction effect). Based on both Range Analysis and Analysis of Variance, it is shown that F, D, Angle and F*D_1 are the import factors that influence the directivity of the LCR wave and their order of importance is Angle>D>F>F*D_1(Interaction effect).

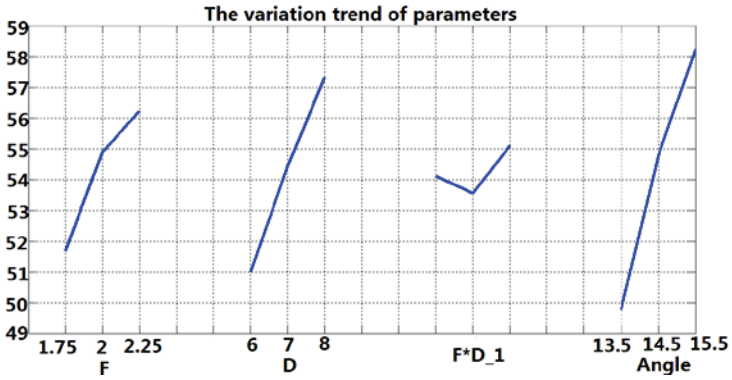

FIGURE 8. The variation trend of important parameters.

Figure 8 shows the variation trend for these important parameters: as the value of each parameter is increased, the directivity of the LCR wave increases to 90^o. In order to increase the directivity of LCR wave to 90^o, the value of the parameters should be increased. As shown above, there are interaction effects between F (frequency of the transducer) and D (the aperture of the transducer). Table 6 is the Binary Table [16] of F and D, which shows their contribution to the directivity with different values.

TABLE 6. Binary Table.

D\F	1.75	2	2.25
6	48	51.333	53.667
7	51	55.667	56.667
8	56	57.667	58.333

Figure 9 is a Biplot Mapping [16] corresponding to the data in the Binary Table. It visualizes the trends in variation more clearly. As shown in the figure, the directivity can reach nearly 60^o when the value of D is 8mm and the value of frequency is 2.25MHz.

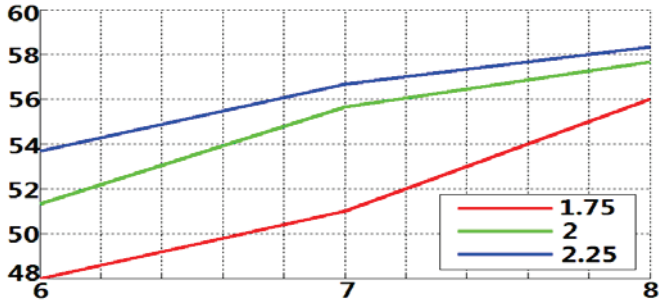

FIGURE 9. Biplot Mapping of F and D.

CONCLUSIONS

The effects of transducer and system configuration for the generation of the LCR or creeping wave have been studied. A new MATLAB based model using a Spatial Fourier Analysis method is reported, that was in good general agreement with more complex and previously published models. The model was used to investigate the effect of

various parameters on the directivity of the LCR wave. The Orthogonal Experiment Method is used to analysis the effects of parameters as seen in the model data. The data show that F (the frequency of the transducer), D (the aperture of the transducer), α (the incident angle) and F*D (the interactive of F and D) all influence the directivity of the LCR wave and their order of significance is Angle>D>F>F*D (Interaction effect). This model data provide insights into the penetration of the wave into a sample.

ACKNOWLEDGEMENTS

This article was supported by China Scholarship Council and the Center for NDE, Iowa State University.

REFERENCES

1. E. H. Dowell, G. F. Gorman III, and D. A.Smith, "Acoustoelasticity: General theory, acoustic natural modes and forced response to sinusoidal excitation, including comparisons with experiment," *Journal of Sound and Vibration*, **52** (4), 519-542 (1997).
2. D. M. Egle and D. E. Bray,"Measurement of acoustoelastic and third-order elasticconstants for rail steel," *J. Acoust. Soc. Am*, **60** (3), 741–744 (1976).
3. F. A. Kandil, J. D. Lord, A. T. Fry, and P. V. Grant, "A Measurement Methods---A Guide to Technique Selection," Report No. MATC (A) 04, National Physical Laboratory, UK.
4. G. S. Schajer and M. Tootoonian, "A New Rosette Design for More Reliable Hole-drilling Residual Stress Measurements," *Experimental Mechanics*, **37** (3), 299-306 (1997).
5. D. S. Hughes and J. L. Kelly, "Second-Order Elastic Deformation of Solids," *Physical Review*, **92** (5), 1145-119 (1953).
6. D. R. Allen and C. M. Sayers, "The measurement of residual stress in textured steel using an ultrasonic velocity combinations technique," *Ultrasonics*, **22** (4), 179-188 (1984).
7. M. Duquennoy, M. Ouaftouh, M. Ourak, and F. Jenot, "Theoretical determination of Rayleigh wave acoustoelastic coefficients: comparison with experimental values," *Ultrasonics*, **39** (8), 575-583 (2002).
8. K. J. Langenberg, P. Fellenger and R. Marklein, "On the nature of the so-called subsurface longitudinal wave and/or the surface longitudinal 'creeping' wave," *Res. Nondestruct. Eval*, **2** (2), 59–81 (1990).
9. F Belahcene and J Lu, "Determination of residual stress using critically refracted longitudinal waves and immersion mode," *Journal of Strain Analysis*, **37** (1), 13-20 (2002).
10. Santos, A. A., Andrino, M. H., Bray D. E., and Trevisan, R. E., "Evaluation of Stresses Generated by Welding in API 5L X65 Steel using Acoustoelasticity," *Materials Evaluation*, **66** (8), 858-864 (2008).
11. Don E.Bray and Paul Junghans,"Application of the Lcr ultrasonic technique for evaluation of post-weld heat treatment in steel plate," *NDT&E International*, **28** (4), 235-242 (1995).
12. F Belahcene and J Lu, "Determination of residual stress using critically refracted longitudinal waves and immersion mode," *Journal of Strain Analysis*, **37** (1), 13-20 (2002).
13. Don E. Bray and Wei Tang, "Subsurface stress evaluation in steel plates and bars using the Lcr ultrasonic wave," *Nuclear Engineering and Design*, **207** (2), 231-240 (2001).
14. H. Lu, X. S. Liu, J. G. Yang, S. P. Zhang and H. Y. Fang, "Ultrasonic tress evaluation on welded plates with Lcr wave," Science and Technology of Welding and Joining, **13**(1), 70-74 (2008).
15. L.V. Basatskaya and I.N. Ermolov, "Theoretical analysis of ultrasonic longitudinal undersurface waves in solid medium," *Sov. J. Nondestruct. Test*, **16** (7), 524–530 (1981).
16. Shanghai Science and Technology Station. The Method of the Orthogonal Experiment Design---multi-factors Experiment Method. Shanghai: *Shanghai People's Press*; 1975.
17. Ying Chen, Jiafan Zhang, Canjun Yang and Bin Niu, "The workspace mapping with deficient-DOF space for the PUMA 560 robot and its exoskeleton arm by using orthogonal experiment design method," *Robotics and Computer-Integrated Manufacturing*, **23** (4) 478-487 (2007).
18. J. L. Lin and C. L. Lin, "The use of the orthogonal array with grey relational analysis to optimize the electrical discharge machining process with multiple performance characteristics," *Machine Tools & Manufacture*, **42**, 237-244 (2002).
19. Kyoji Matsushima and Tomoyoshi Shimobaba, "Band-limited Angular Spectrum Method for Numerical Simulation of Free-Space Propagation in Far and Near Fields," *Optics Express*, **17** (2), 19662-19673 (2009).

20. Djema Belgroune, Jean Francois de Belleval and Hakim Djelouah, "A theoretical study of ultrasonic wave transmission through a fluid-solid interface," *Ultrasonics*, **48** (3), 220-230 (2008).
21. S. Chaki, W. Ke and H. Demouveau, "Numerial and experimental analysis of the critically refracted longitudinal beam," *Ultrasonics*, **53** (1), 65-69 (2013).
22. Wenguo Cui, Xiaohong Li, Shaobing Zhou, and Jie Weng, "Investigation on process parameters of electrospinning system through orthogonal experimental design," *Applied Polymer*, **103** (5), 3105-3112 (2007).